# Sequence-Specific Binding of a Hormonally Regulated mRNA Binding Protein to Cytidine-Rich Sequences in the Lutropin Receptor Open Reading Frame†

John C. Kash‡ and K. M. J. Menon*

*Departments of Biological Chemistry and Obstetrics/Gynecology, University of Michigan Medical School, Ann Arbor, Michigan 48109-0617*

*Received July 8, 1999; Revised Manuscript Received September 21, 1999*

ABSTRACT: In previous studies, a lutropin receptor mRNA binding protein implicated in the hormonal regulation of lutropin receptor mRNA stability was identified. This protein, termed LRBP-1, was shown by RNA gel electrophoretic mobility shift assay to specifically interact with lutropin receptor RNA sequences. The present studies have examined the specificity of lutropin receptor mRNA recognition by LRBP-1 and mapped the contact site by RNA footprinting and by site-directed mutagenesis. LRBP-1 was partially purified by cation-exchange chromatography, and the mRNA binding properties of the partially purified LRBP-1 were examined by RNA gel electrophoretic mobility shift assay and hydroxyl-radical RNA footprinting. These data showed that the LRBP-1 binding site is located between nucleotides 203 and 220 of the receptor open reading frame, and consists of the bipartite polypyrimidine sequence 5′-UCUC-$X_7$-UCUCCCU-3′. Competition RNA gel electrophoretic mobility shift assays demonstrated that homoribopolymers of poly(rC) were effective RNA binding competitors, while poly(rA), poly(rG), and poly(rU) showed no effect. Mutagenesis of the cytidine residues contained within the LRBP-1 binding site demonstrated that all the cytidines in the bipartite sequence contribute to LRBP-1 binding specificity. Additionally, RNA gel electrophoretic mobility supershift analysis showed that LRBP-1 was not recognized by antibodies against two well-characterized poly(rC) RNA binding proteins, αCP-1 and αCP-2, implicated in the regulation of RNA stability of α-globin and tyrosine hydroxylase mRNAs. In summary, we show that partially purified LRBP-1 binds to a polypyrimidine sequence within nucleotides 203 and 220 of lutropin receptor mRNA with a high degree of specificity which is indicative of its role in posttranscriptional control of lutropin receptor expression.

A key event in the regulation of steroidogenesis in the mammalian ovary is the interaction of luteinizing hormone (LH), or its human placental counterpart human chorionic gonadotropin (hCG), with the lutropin receptor (*1*). The lutropin receptor belongs to the family of $G_s$-protein-coupled receptors that mediate their biological effects through cAMP production (*2*). Lutropin receptors expressed on the ovarian granulosa cells and luteal cells are greatly diminished by an endogenous preovulatory LH surge, or by the administration of a pharmacological dose of hCG (*3*). Previous studies from our laboratory have shown that the decline in cell surface lutropin receptor number that occurs during hCG-induced down-regulation is paralleled by a specific loss of lutropin receptor mRNA (*4*, *5*). Following the injection of a bolus of hCG in female rat, a rapid decline in the steady-state levels of all four of the lutropin receptor mRNA transcripts (6.7, 4.4, 2.6, and 1.8 kb) is seen within 12 h, with complete loss of detectable receptor mRNAs by 24 h. This selective loss is followed by a recovery of mRNA expression between 24 and 48 h (*4*, *5*). We have further reported that loss of receptor mRNA does not result from decreased transcription, but occurs posttranscriptionally, with an approximate 3-fold decrease in receptor mRNA half-life (*6*).

The steady-state level of a mRNA, in general, is determined by the balance between the rates of synthesis and degradation. The rate of mRNA degradation, in turn, can be mediated by the dynamic interactions of specific RNA binding proteins, as reported in many systems, including cytokines, oncogenes, and G-protein-coupled receptors (*7*−*15*). Attempts are currently underway to identify specific regulatory elements and trans-acting factors that participate in the regulated degradation of specific mRNAs.

To study the molecular basis of the posttranscriptional control of lutropin receptor mRNA, we identified two proteins which bound sequences located between nucleotides 102 and 282 of the receptor open reading frame by RNA gel electrophoretic mobility shift analysis (*16*). Incubation of protein extracts from control and hormone-treated (down-regulated) rat ovary with radiolabeled lutropin receptor mRNAs showed the formation of two sequence-specific ribonucleoprotein (RNP) complexes of approximately 50 and 45 kDa, termed LRBP-1 and LRBP-2, respectively. Both LRBP-1 and LRBP-2 were shown to bind in the lutropin receptor open reading frame. Moreover, the RNA binding activity of LRBP-1 was further demonstrated to be regulated

† Supported by NIH Grant HD-06656.

* Address correspondence to this author at 6428 Medical Sciences Building I, 1301 Catherine St., Ann Arbor, MI 48109-0617. Telephone 734-764-8142, Fax 734-936-8617.

‡ Predoctoral fellow supported by NIH Training Grant PR5-T32-HD-07048.

10.1021/bi9915770 CCC: $18.00 
Published on Web 12/01/1999

by hCG and increased ~3-fold during lutropin receptor down-regulation (*16*).

To characterize the interaction of LRBP-1 with lutropin receptor mRNA, LRBP-1 was partially purified using cation-exchange chromatography. The sequence specificity of LRBP-1 eluted from an S-Sepharose column was characterized by RNA electrophoretic mobility shift and hydroxyl-radical RNA footprinting analyses. The data presented here demonstrate that the LRBP-1 binds a cytidine-rich bipartite sequence in the lutropin receptor open reading frame composed of nucleotides 5′-$U_{203}$CUC-$X_7$-UCUCCC$U_{220}$-3′, with a low apparent equilibrium dissociation constant. These data demonstrate a high degree of specificity in the interaction of LRBP-1 with lutropin receptor mRNA between nucleotides 203 and 220, and suggest a role for LRBP-1 in determining the specificity of hCG-regulated turnover of lutropin receptor mRNA in the rat ovary.

## MATERIALS AND METHODS

*Animals and Tissues.* Twenty-one day old Sprague-Dawley female rats were injected subcutaneously with 50 IU pregnant mare serum gonadotropin (Calbiochem), followed by 25 IU human chorionic gonadotropin (hCG; Sigma) 56 h later to induce superovulation. Lutropin receptor down-regulation was induced by the injection of 50 IU of hCG 5 days later, as previously described (*4*−*6*, *16*). Ovaries were collected 12 h following the final hCG injection and were either processed immediately or stored in liquid nitrogen until use.

*Partial Purification of LRBP-1.* Ovaries were homogenized at 4 °C in buffer A (10 mM HEPES, pH 7.9, 0.5 mM $MgCl_2$, 50 $\mu$M EDTA, 5 mM DTT, 10% glycerol) containing 50 mM KCl and EDTA-free complete protease inhibitor cocktail (Boehringer Mannheim) followed by centrifugation at 105000*g* for 90 min at 4 °C. The supernatants (S100) were collected, and proteins were quantified by bicinchoninic acid assay (BCA) (Pierce Chemical Co.). The S100 fractions were applied to an S-Sepharose column (BioRad) (5 mg of protein/mL of packed chromatography resin) equilibrated with 20 bed volumes of buffer A (without protease inhibitors), and the column effluent was monitored continuously by measuring the absorbance at 280 nm. The column was washed until the absorbance at 280 nm was less than 0.02 (approximately 10 bed volumes). The proteins were eluted with buffer A containing a stepwise KCl gradient (150−500 mM). S-Sepharose column eluates were desalted to 50 mM KCl in buffer A, plus EDTA-free complete protease inhibitor cocktail, using Centriprep-10 micro-concentrators (Amicon), and protein concentrations were determined by BCA.

*Preparation of RNAs.* Lutropin receptor cDNA nucleotides 102−282 (LR:102−282 cDNA) was prepared by partial digestion of a full-length rat lutropin receptor cDNA and cloning into the pBluescript II vector (Stratagene), as previously described (*16*). The cDNAs used to generate wild-type and mutant (see Figure 9, panel A) LR:188−228 RNAs were chemically synthesized, and contained the T7 RNA polymerase promoter at the 5′ end. A lutropin receptor cDNA containing nucleotides 711−1401 was prepared by directional cloning of an *Acc*I, *Apa*I fragment of a 2.2 kb full-length open reading frame cDNA (*17*), and was used to generate LR:711−1401 RNA. A full-length human glyceraldehyde-3-phosphate dehydrogenase (GAPDH) cDNA was obtained from ATCC (*18*). The nomenclature used throughout this report to describe lutropin receptor RNAs designates nucleotide 1 as the first nucleotide transcribed in the 5′-untranslated region of the 2.2 kb cDNA (*17*).

RNAs were prepared from linearized cDNA templates using the Maxiscript and Megashortscript kits according to the manufacturer (Ambion), and essentially as described by Melton et al. (*19*). For uniformly radiolabeled RNAs, transcription reactions were performed in the presence 100 $\mu$Ci of [$\alpha$-$^{32}$P]UTP (800 Ci/mmol; NEN) without additional unlabeled UTP. Following transcription, RNAs were treated with RNase-free DNase I and were extracted with water-saturated phenol−chloroform−isoamyl alcohol (50:49:1). Unincorporated nucleotides were separated from the labeled RNA using Nuc-Trap columns (Stratagene). RNA was then precipitated with 2.5 volumes of ethanol and 0.1 volume of 3 M sodium acetate, pH 5.4. The RNA was reconstituted in buffer containing 1 mM EDTA and was stored at −20 °C. To prepare 5′ end labeled LR:188−228 RNA, in vitro transcribed RNAs were then gel-purified on a 2% agarose gel (NuSieve GTG agarose; FMC) and were electroeluted at 200 V for 15 min (IBI), followed by ethanol precipitation. 5′ end labeled RNAs were prepared by dephosphorylation of 200 pmol of RNA with 20 units of calf intestinal phosphatase at 50 °C for 90 min and with an additional 10 units of phosphatase for 30 min (*20*). RNAs were extracted twice with water-saturated phenol−chloroform−isoamyl alcohol (50:49:1) and were precipitated with 2.5 volumes of ethanol and 0.1 volume of 3 M sodium acetate, pH 5.4. The RNAs were then labeled with T4 polynucleotide kinase (New England Biolabs) and 1.0 mCi of [$\gamma$-$^{32}$P]ATP (6000 Ci/mmol; NEN) (*20*). Radiolabeled RNAs were gel-purified by 8 M urea/20% polyacrylamide gel electrophoresis, and eluted in 2 M ammonium acetate, 1% SDS, and 0.5 mg/mL yeast tRNA overnight at 25 °C. Radiolabeled RNAs were quantified by liquid scintillation counting, and unlabeled RNAs were quantified by measurement of the absorbance at 260 nm. Radiolabeled RNA concentrations were calculated by the specific activity of the incorporated radiolabeled nucleotide.

*RNA Gel Shift Analysis.* Unless otherwise indicated, RNA gel shift analysis was performed as described previously (*16*). Briefly, protein samples were incubated with $1 \times 10^5$ cpm of radiolabeled, gel-purified RNA in homogenization buffer (described above) in the presence of 5 $\mu$g of tRNA and 40 units of RNasin (Promega) at 30 °C for 10 min. Unprotected radiolabeled RNA was then degraded by the addition of 2 units of RNase T1 (Boehringer Mannheim) at 37 °C for 30 min. When indicated, unlabeled competitor RNAs were also included in the binding reaction. Samples were then incubated with heparin at a final concentration of 5 mg/mL for 10 min on ice to decrease nonspecific binding. The RNA−protein complexes were resolved by 8% native polyacrylamide gel electrophoresis at 4 °C. The gel was then dried and exposed to Kodak XAR film and visualized by autoradiography. RNA gel electrophoretic mobility shift analysis was also performed by incubation of $(2.5-5) \times 10^4$ cpm of radiolabeled LR:188−228 RNA with 2.5−5 $\mu$g of the 150 mM S-Sepharose for 15 min at 30 °C, followed by 5% native polyacrylamide gel electrophoresis for 3 h at 4 °C. The radiolabeled bands on the gel were visualized by autoradiography. When indicated, quantification of radiolabeled

bands was performed using a phosphorimager and ImageQuant software (Molecular Dynamics). RNA supershift analysis was performed by incubation of $2.5 \times 10^4$ cpm of radiolabeled, gel-purified LR:188−288 with 2 $\mu$g of 150 mM KCl S-Sepharose eluate or 40 $\mu$g of the supernatant of a 130000*g* (S130) from pheochromocytoma-derived PC12 cells (where indicated) for 15 min at 30 °C, and were then incubated with polyclonal antibodies specific for αCP-1 (*21*) or αCP-2 (*22*) for 1 h at 4 °C, followed by separation by polyacrylamide gel electrophoresis on 5% native gels.

*RNA Footprinting.* Hydroxyl-radical [Fe(II)-EDTA] RNA footprinting was performed essentially as described previously (*20*). Briefly, $5 \times 10^5$ cpm of gel-purified, 5′ end labeled RNA was incubated with 50−400 $\mu$g of 150 mM KCl S-Sepharose eluate of LRBP-1 in buffer containing 10 mM sodium phosphate buffer (pH 6.5), 50 mM NaCl, 1 mM EDTA, and 0.15 mg/mL yeast tRNA for 30 min at room temperature. RNA strand scission was performed by the addition of freshly prepared solutions of 2 mM Fe(II) (Aldrich)/4 mM EDTA and 10 mM DTT (final concentration), followed by incubation at room temperature for 60 min. The reaction was quenched by the addition of thiourea (10 mM final) and incubation for 5 min at room temperature. Cleavage reactions were then extracted with phenol−chloroform−isoamyl alcohol (50:49:1) and were ethanol-precipitated in the presence of 5 $\mu$g of yeast tRNA at −80 °C. Samples were washed with 75% ethanol, dried, and resuspended in loading buffer (95% formamide, 10 mM EDTA, 0.05% xylene cyanol, 0.05% bromophenol blue, and 0.1% SDS), and an equal number of counts were incubated at 68 °C for 5 min, immediately prior to electrophoresis. RNA hydrolysis standards were prepared by digestion of 5′ end labeled LR:188−228 RNA with 1−3 units of RNase T1 under denaturing conditions (25 mM citrate, pH 4.8, 1 mM EDTA, and 7 M urea) for 15 min at 50 Ci and by limited alkaline hydrolysis with incubation in 50 mM $Na_2CO_3$, pH 11.7, at 95 °C for 30−90 s, followed by rapid quench with 25 mM citrate, pH 4.8, and 10 M urea. The RNA cleavage products were then resolved by 8 M urea/20% polyacrylamide gel electrophoresis at 60 W for 4 h. The gel was fixed with 10% acetic acid and 10% methanol, and the RNA cleavage products were visualized by autoradiography.

## RESULTS

*Partial Purification of LRBP-1 Using Cation-Exchange Chromatography.* To characterize the interaction of LRBP-1 with lutropin receptor, LRBP-1 was partially purified using cation-exchange chromatography on an S-Sepharose matrix with subsequent elution of proteins in buffer A containing increasing KCl concentrations. Down-regulated ovarian S100 was applied to an S-Sepharose column at 50 mM KCl (pH 7.8) in buffer A plus EDTA-free complete protease inhibitor cocktail and washed extensively, and proteins were eluted with buffer A containing a stepwise KCl gradient (50−500 mM). Samples were desalted in buffer A plus protease inhibitors to 50 mM KCl, quantified, and analyzed by RNA gel mobility shift analysis. As shown in Figure 1, incubation of $1 \times 10^5$ cpm of LR:102−282 with 50 $\mu$g of homogenate or 50 $\mu$g of S100 (lanes 2 and 3) resulted in the appearance of the 50 kDa LRBP-1 and 45 kDa LRBP-2 RNP complexes. However, when S100 was applied to the S-Sepharose column in buffer A containing 50 mM KCl, LRBP-1 was retained

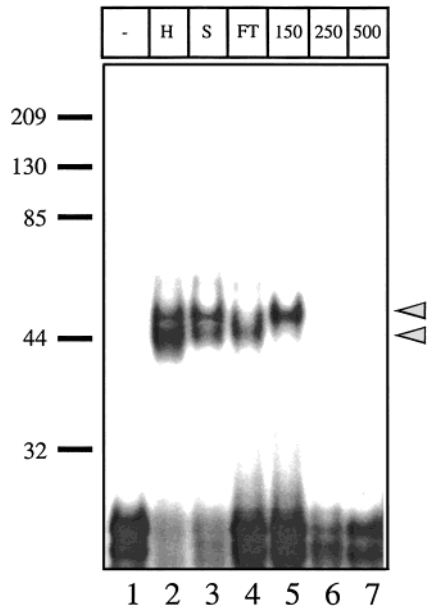


FIGURE 1: Partial purification of LRBP-1 using cation-exchange chromatography. Representative autoradiogram of RNA gel mobility shift analysis performed using $1 \times 10^5$ cpm of LR:102−282 RNA incubated with no protein (lane 1), 50 $\mu$g of homogenate from down-regulated (12 h post-hCG) (lane 2), 50 $\mu$g of S100 (lane 3), 50 $\mu$g of column flow-through (lane 4), or 5 $\mu$g of 150 mM KCl S-Sepharose eluate (lane 5), 5 $\mu$g of 250 mM KCl S-Sepharose elute (lane 6), or 50 $\mu$g of 500 mM KCl S-Sepharose eluate protein (lane 7). The samples were treated with RNase T1, separated by polyacrylamide gel electrophoresis on an 8% native gel, and visualized by autoradiography. This figure is representative of four separate experiments.

on the column which could be eluted with buffer A containing 150 mM KCl (lane 5). Additionally, partial purification of LRBP-1 resulted in an approximate 20-fold enrichment in LRBP-1 RNA binding activity (see Figure 2). The 150 mM KCl S-Sepharose eluate was used in the remainder of the experiments described in this report.

To quantify the enrichment of LRBP-1 RNA binding activity, several concentrations (0.5, 5.0, and 10 $\mu$g) of homogenate (lanes 2−4), S100 (lanes 5−7), or the 150 mM KCl eluate were incubated with $1 \times 10^5$ cpm of LR:102−282 RNA at 30 °C for 10 min, followed by RNase T1 treatment, and the RNP complexes were resolved by 8% native polyacrylamide gel electrophoresis. As shown in Figure 2, cation-exchange chromatography resulted in an enrichment in the LRBP-1 RNA binding activity. Further analysis revealed an approximate 20-fold enrichment in LRBP-1 in the 150 mM KCl S-Sepharose eluate (data not shown).

*Analysis of LRBP-1 RNA Binding Specificity.* To confirm that the lutropin receptor mRNA binding activity contained in the 150 mM KCl S-Sepharose eluate was specific for receptor RNA, a series of competition RNA electrophoretic mobility shift assays were performed by coincubation of radiolabeled LR:102−282 RNA with increasing concentrations of specific and nonspecific unlabeled competitor RNAs. As shown in Figure 3, $1 \times 10^5$ cpm (10 ng) of radiolabeled LR:102−282 RNA was incubated with 5 $\mu$g of 150 mM KCl S-Sepharose eluate in the absence (lanes 2, 6, and 10) or presence of increasing concentrations (0.01, 0.1, or 1 $\mu$g) of LR:102−468 (lanes 3−5), LR:711−1401 (lanes 7−9), or full-length glyceraldehyde-3-phosphate dehydrogenase (GAP-

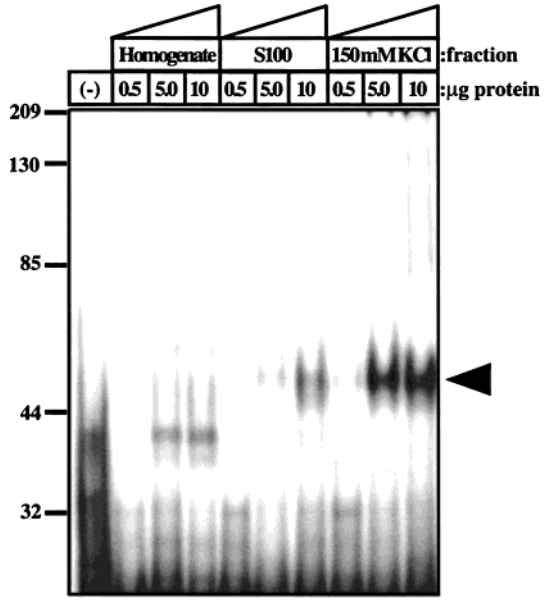


FIGURE 2: Enrichment of LRBP-1 RNA binding activity. Representative autoradiogram of RNA gel mobility shift performed using $1 \times 10^5$ cpm of LR:102−282 RNA incubated with no protein (lane 1), increasing concentrations of S100 (0.5, 5.0, and 10 $\mu$g) (lanes 2−4), or increasing concentrations (0.5, 5.0, and 10 $\mu$g) of the 150 mM KCl S-Sepharose eluate (lanes 5−7). The samples were treated with RNase T1, separated by polyacrylamide gel electrophoresis on an 8% native gel, and visualized by autoradiography. These data are representative of three separate experiments.

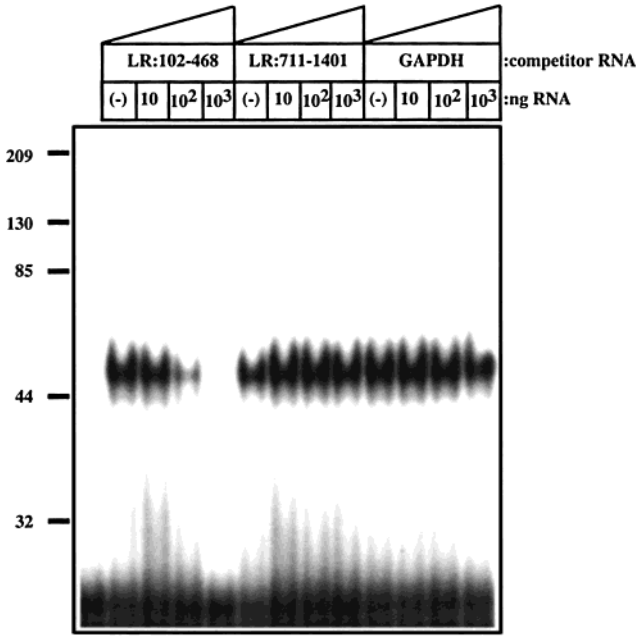


FIGURE 3: LRBP-1 RNA binding specificity. Representative autoradiogram of RNA gel mobility shift analysis performed using $1 \times 10^5$ cpm of LR:102−282 RNA (10 ng) incubated without protein (lane 1) or with 5 $\mu$g of 150 mM KCl S-Sepharose eluate in the presence of increasing concentrations (0, 10, 100, or 1000 ng) of cold competitor RNAs: LR:102−468 (lanes 2−5), LR:711−1401 (lanes 6−9), or glyceraldehyde-3-phosphate dehydrogenase (GAPDH) RNAs. The samples were treated with RNase T1, separated by polyacrylamide gel electrophoresis on an 8% native gel, and visualized by autoradiography. These data are representative of three separate experiments.

DH) (lanes 11−13) RNAs. This analysis demonstrated that the enriched LRBP-1 still displayed the sequence-specific RNA binding activity we have previously reported.

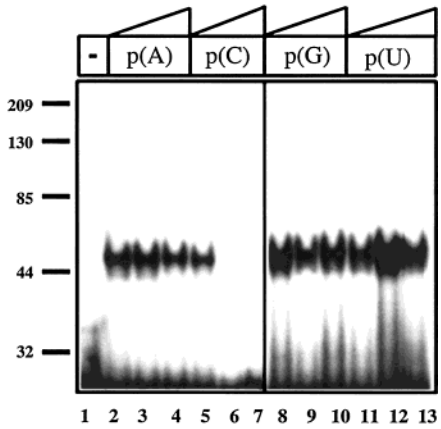


FIGURE 4: Poly(rC) RNA competes for LRBP-1 binding. Representative autoradiogram of RNA gel mobility shift analysis performed using $1 \times 10^5$ cpm of LR:102−282 RNA (10 ng) incubated without protein (lane 1) or with 5 $\mu$g of 150 mM KCl S-Sepharose eluate in the presence of increasing concentrations (1-, 10-, and 100-fold molar excesses) of unlabeled homoribopolymers of poly(rA) (lanes 2−4), poly(rC) (lanes 5−7), poly(rG) (lanes 8−10), and poly(rU) (lanes 11−13). The samples were treated with RNase T1, separated by polyacrylamide gel electrophoresis on an 8% native gel, and visualized by autoradiography. These data are representative of three separate experiments.

To determine if LRBP-1 displayed a preference for any single nucleotide, competition RNA gel electrophoretic mobility shift analysis was performed with homoribopolymers of poly(rA), poly(rC), poly(rG), and poly(rU). As shown in Figure 4, $1 \times 10^5$ cpm (10 ng) of radiolabeled LR:102−282 RNA was incubated with 5 $\mu$g of the partially purified LRBP-1 in the 150 mM KCl S-Sepharose eluate in the absence (lanes 2, 5, 8, and 11) or presence of increasing concentrations (10- or 100-fold molar excess) of unlabeled poly(rA) (lanes 3, 4), poly(rC) (lanes 6, 7), poly(rG) (lanes 9, 10), or poly(rU) (lanes 12, 13) RNAs. This analysis demonstrated that LRBP-1 binding could be completed only by poly(rC) RNA, and suggested that cytidine residues are important components of the LRBP-1 RNA binding site.

*Determination of the LRBP-1 Binding Site.* To determine the LRBP-1 binding site on lutropin receptor RNA, RNase T1 RNA footprinting analysis was initially performed and suggested that LRBP-1 bound between nucleotides 188 and *288* of the lutropin receptor open reading frame (data not shown). Based on these data, a cDNA containing nucleotides 188−228 with the T7 RNA polymerase promoter at the 5′ end was prepared by chemical synthesis. This cDNA was used to prepare radiolabeled LR:188−228 RNA, which was then used for RNA gel electrophoretic mobility shift analysis. Increasing concentrations of 150 mM KCl S-Sepharose eluate (2.5−20 $\mu$g) were incubated with $1 \times 10^5$ cpm of LR:188−228 RNA, treated with RNase T1, and separated by polyacrylamide gel electrophoresis on 8% native gels. As shown in Figure 5, panel A, incubation of increasing concentrations of 150 mM KCl S-Sepharose eluate with radiolabeled LR:188−228 RNA resulted in a concentration-dependent increase in formation of the ~50 kDa radiolabeled RNP complex. These data demonstrated that the sequences between nucleotides 188 and *228* of lutropin receptor mRNA were sufficient to bind to LRBP-1.

To ensure that interaction of LRBP-1 with the LR:188−228 RNA was sequence-specific, competition RNA gel electrophoretic mobility shift analysis was performed by

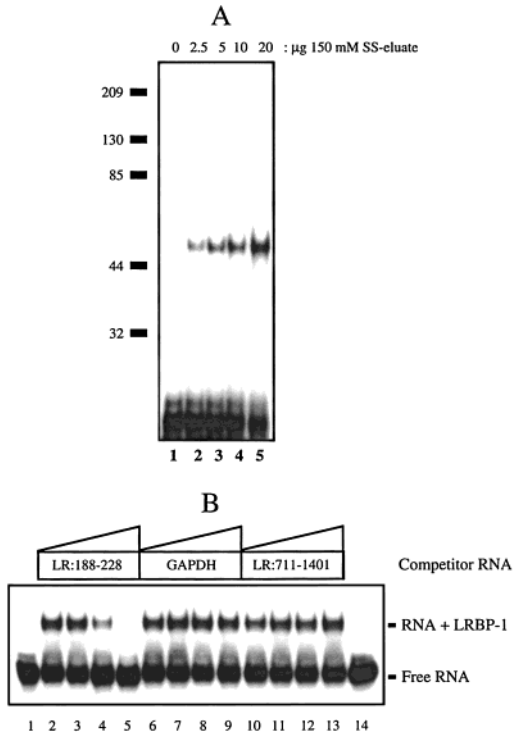


FIGURE 5: (A) Determination of the LRBP-1 lutropin receptor mRNA binding site to nucleotides 188−228 of lutropin receptor mRNA. Representative autoradiogram of RNA gel mobility shift analysis performed by incubation of $1 \times 10^5$ cpm of LR:188−228 RNA in the absence (lane 1) or presence of increasing concentrations [2.5 $\mu$g (lane 1), 5 $\mu$g (lane 2), 10 $\mu$g (lane 3), or 20 $\mu$g (lane 4)] of 150 mM KCl S-Sepharose eluate. The samples were treated with RNase T1, separated by polyacrylamide gel electrophoresis on an 8% native gel, and visualized by autoradiography. These data are representative of two separate experiments. (B) Competition of LRBP-1 binding to LR:188−228 RNA. Representative autoradiogram of RNA gel mobility shift analysis performed by incubation of $5 \times 10^4$ cpm of LR:188−228 RNA alone (lanes 1 and 14) or with 5 $\mu$g of 150 mM KCl S-Sepharose eluate in the absence or presence of increasing concentrations of unlabeled competitor RNAs: LR:188−228 (lanes 2−5), GAPDH (lanes 6−9), or LR:711−1401 RNA (lanes 10−13). The samples were then resolved by polyacrylamide gel electrophoresis on a 5% native gel at 75 V for 3 h at 4 °C. These data are representative of two separate experiments.

incubating 5 $\mu$g of the 150 mM KCl S-Sepharose eluate with radiolabeled LR:188−228 RNA in the absence and presence of increasing concentrations of unlabeled competitor RNAs. Because the molecular mass of the LR:188−228 RNA was small (10 463 Da), separation of free radiolabeled LR:188−228 RNA from the 50 kDa radiolabeled LR:188−228/LRBP-1 RNP complex could be accomplished by native polyacrylamide gel electrophoresis, without the need for RNase T1 treatment. As shown in Figure 5, panel B, $5 \times 10^4$ cpm (0.32 ng) of radiolabeled LR:188−228 RNA was incubated with 5 $\mu$g of the 150 mM KCl S-Sepharose eluate for 30 min at 30 °C in the absence and presence of increasing concentrations (0-, 1-, 10-, and 100-fold molar excesses) of unlabeled LR:188−228 (lanes 2−5), GAPDH (lanes 6−9), or LR:711−1401 RNA (lanes 10−13), followed by polyacrylamide gel electrophoresis on a 5% native gel for 3 h at 4 °C. This analysis demonstrated that only LR:188−228 RNA competed for LRBP-1 binding, while the GAPDH and LR:711−1401 RNAs showed no effect on LRBP-1 binding of radiolabeled LR:188−228 RNA.

To obtain an estimate of the apparent $K_d$ for the binding of LRBP-1 to LR:188−228 RNA, increasing amounts of radiolabeled LR:188−228 RNA (0.1, 0.2, 1.2, and $2.4 \times 10^{-13}$ mol) were incubated with 2 $\mu$g of the 150 mM KCl S-Sepharose eluate for 30 min at 30 °C, followed by polyacrylamide gel electrophoresis on a 5% native gel, as shown in Figure 6, panel A. The radiolabeled species were analyzed using a phosphorimager (Molecular Dynamics), and the concentrations of free and bound LR:188−228 RNA were measured using the ImageQuant densitometry software (Molecular Dynamics) and from the specific activity of the radiolabeled RNA. Scatchard analysis was performed, and an apparent $K_d$ was determined to be approximately 4 nM (panel B). These data demonstrated that LRBP-1 specifically bound sequences contained between nucleotides 188 and 228 of the lutropin receptor mRNA.

*Hydroxyl-Radical RNA Footprinting.* To identify the base contacts made by LRBP-1, hydroxyl-radical RNA footprinting analysis was performed. To perform RNA footprinting, the concentration of 150 mM S-Sepharose eluate required to bind >50% of the gel-purified, 5′ end labeled LR:188−

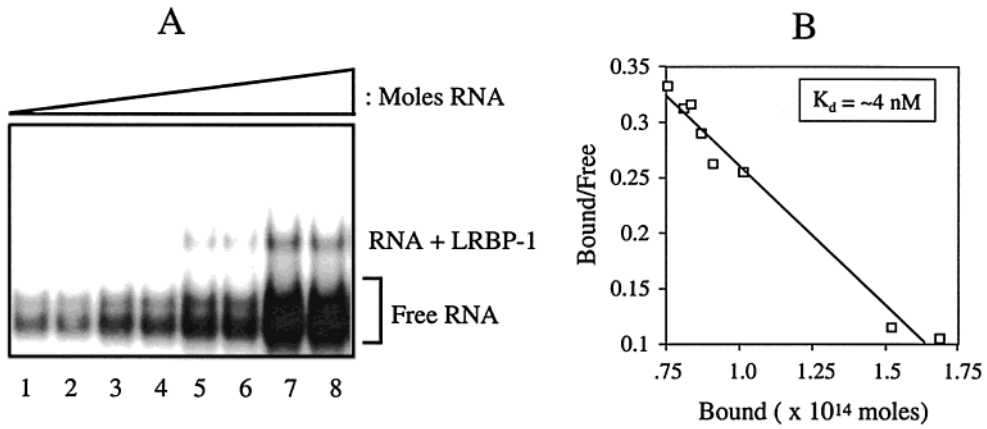


FIGURE 6: Determination of the apparent LRBP-1 equilibrium dissociation constant of LRBP-1 binding to LR:188−228 RNA. Panel A: representative autoradiogram of RNA gel mobility shift analysis performed by incubation of 2 $\mu$g of 150 mM KCl S-Sepharose eluate incubated with increasing amounts [$0.1 \times 10^{-13}$ (lanes 2, 3), $0.2 \times 10^{-13}$ (lanes 4, 5), $1.2 \times 10^{-13}$ (lanes 6, 7), or $2.4 \times 10^{-13}$ (lanes 8, 9) mol] of radiolabeled LR:188−228 RNA in 0.01 mL final volume. The samples were then resolved by polyacrylamide gel electrophoresis on a 5% native gel at 75 V for 3 h at 4 °C. Quantification of the gel was performed using a phosphorimager and ImageQuant densitometry software (Molecular Dynamics). Panel B: Scatchard analysis of the data presented in panel A. The apparent $K_d$ of LRBP-1 binding was approximately 4 nM. These data are representative of two separate experiments.

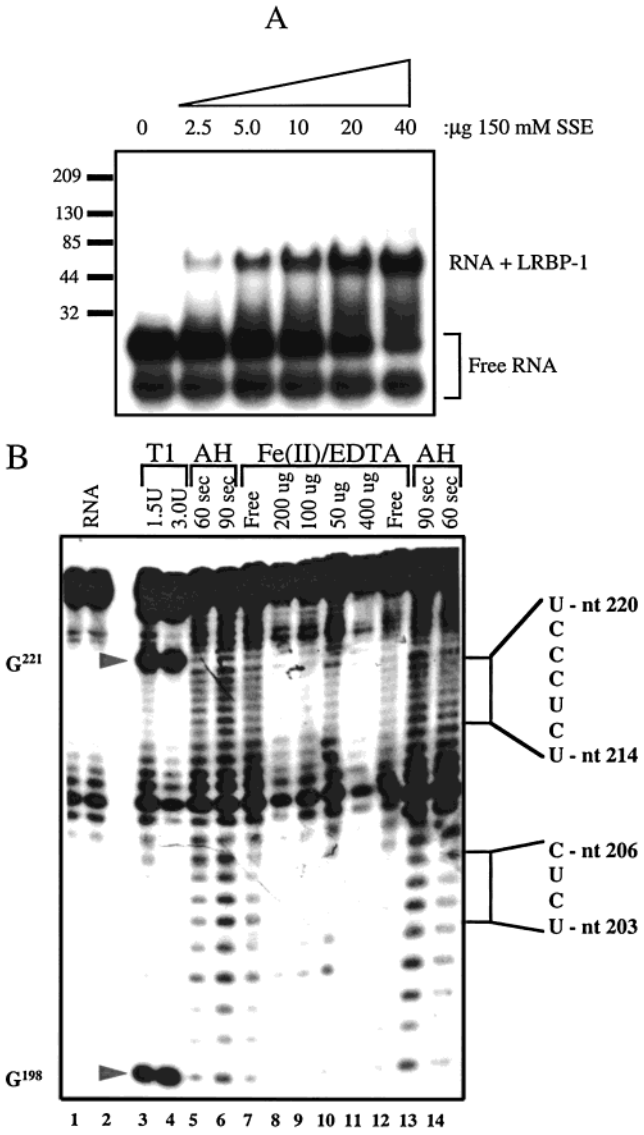


FIGURE 7: Hydroxyl-radical RNA footprinting of LR:188−228 RNA incubated with LRBP-1. Panel A: representative autoradiogram of the titration of 5′ end labeled RNA with the 150 mM KCl S-Sepharose eluate by electrophoretic mobility shift analysis performed by incubation of $5 \times 10^4$ cpm of LR:188−228 RNA in the absence (lane 1) or presence of increasing concentrations [2.5 $\mu$g (lane 2), 5 $\mu$g (lane 3), 10 $\mu$g (lane 4), 20 $\mu$g (lane 5), or 40 $\mu$g (lane 6)] of 150 mM KCl S-Sepharose eluate in RNA footprinting buffer followed by 5% native polyacrylamide gel electrophoresis at 100 V for 3 h at 4 °C. Panel B: representative autoradiogram of hydroxyl-radical RNA footprinting analysis performed by incubation of $5 \times 10^5$ cpm of 5′ end labeled LR:188−228 RNA incubated in the absence or presence of increasing concentrations of the 150 mM KCl S-Sepharose eluate, followed by hydroxyl-radical strand cleavage initiated by incubation with Fe(II)/EDTA and DTT. Nucleotide positions were determined by comparison to RNase T1 (lanes 3, 4) and limited alkaline hydrolysis standards (lanes 5, 6 and 13, 14). These data are representative of two separate experiments.

228 RNA was determined by RNA electrophoretic mobility shift analysis. As shown in Figure 7, panel A, $5 \times 10^4$ cpm of LR:188−228 RNA was incubated in the absence (lane 1) or presence of increasing concentrations (2.5−40 $\mu$g) of 150 mM KCl S-Sepharose eluate in hydroxyl-radical footprinting buffer containing 10 mM sodium phosphate, pH 6.8, 50 mM NaCl, 1 mM EDTA, and 0.15 mg/mL yeast tRNA for 30 min at room temperature, followed by polyacrylamide gel

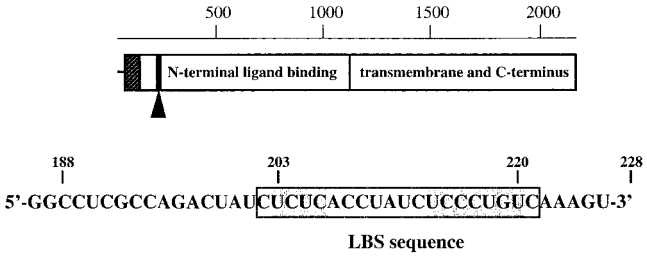


FIGURE 8: Diagram of the LRBP-1 RNA binding site. Diagram of the lutropin receptor mRNA open reading frame showing the position of the LRBP-1 binding site (LBS). The sequence of the LR:188−228 RNA is also shown, with the nucleotides protected from hydroxyl-radical cleavage indicated by the shaded boxes.

electrophoresis on a 5% native gel at 75 V for 3 h at 4 °C. The results (Figure 7, panel A) show that greater than 50% of the radiolabeled LR:188−228 was bound at concentrations of 20 and 40 $\mu$g of the SSE fraction.

Hydroxyl-radical footprinting was performed using a previously published procedure (*20*). Briefly, RNA binding reactions were prepared by incubation of $5 \times 10^5$ cpm of gel-purified, 5′ end labeled LR:188−288 RNA with increasing concentrations of 150 mM KCl SSE (50, 100, 200, and 400 $\mu$g) in footprinting buffer (described above) for 30 min at room temperature. The RNA cleavage reaction was performed by the addition of 2 mM Fe(II)/4 mM EDTA, and 10 mM DTT followed by incubation at room temperature for 60 min. The cleavage reactions were quenched by the addition of thiourea and were extracted with phenol−chloroform and ethanol-precipitated. Equal amounts of radioactivity were then separated by denaturing 20% polyacrylamide gel electrophoresis at 60 W for 4 h. Nucleotide positions were determined by digestion of 5′ end labeled LR:188−228 RNA with RNase T1 (lanes 3, 4) and limited alkaline hydrolysis standards (lanes 5, 6 and 13, 14).

As shown in Figure 7, panel B, incubation of 5′ end labeled LR:188−228 RNA with increasing concentrations of 150 mM KCl S-Sepharose eluate (lanes 8−11) resulted in the increased protection of two prominent regions (located between nucleotides 203−206 and 214−220) from hydroxyl-radical strand cleavage, compared to RNA incubated without LRBP-1 (lanes 8−11). These lanes additionally show limited protection of nucleotides upstream to nucleotide 203 which may be due to nonspecific RNA−protein interactions as a result of the high concentrations of protein used in the footprinting reactions. These data suggested that LRBP-1 protected the sequence 5′-$U_{203}$CUC-$X_7$-UCUCCCU$_{220}$-3′ from cleavage by freely diffusible hydroxyl radicals (shown diagrammatically in Figure 8).

*Mutational Analysis of the LRBP-1 Binding Site (LBS).* To determine the nucleotides critical for LRBP-1 binding, a series of mutant LBS cDNAs were chemically synthesized, and the resultant RNAs, in which specific cytidines were changed to uridine, were used for competition RNA gel electrophoretic mobility shift analysis. Mutant cDNAs with the T7 RNA polymerase promoter at the 5′ end were prepared by chemical synthesis, and RNA was prepared by in vitro transcription, as described under Materials and Methods. The mutant RNAs generated were $C^{204,206}U$, $C^{215,217-219}U$, $C^{217,218}U$, and $C^{204,206,215,217-219}U$, as shown in Figure 9, panel A. In the mutant RNAs, the cytidines in the LBS were mutated because only poly(rC) RNAs were

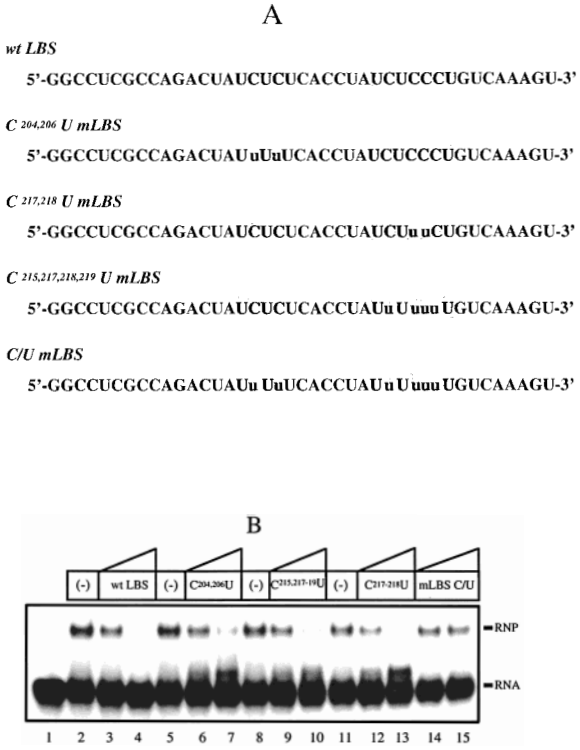


FIGURE 9: Wild-type and mutant LBS RNA sequences. Panel A: diagram of wild-type and mutant LRBP-1 binding site (LBS) RNAs used in RNA electrophoretic mobility shift analysis. Mutations are shown with lower case letters. Panel B: representative autoradiogram of competition RNA gel electrophoretic mobility shift analysis performed by incubation of $5 \times 10^5$ cpm (0.3 ng) of LR:188−228 RNA in the absence (lane 1) or presence of 5 $\mu$g of 150 mM KCl S-Sepharose eluate in the absence (lanes 2, 5, 8, 11) or presence of a 10-fold or 100-fold molar excess of wild-type LBS (lanes 3, 4), mLBS $C^{204,206}U$ (lanes 6, 7), mLBS $C^{215,217-219}U$ (lanes 9, 10), mLBS $C^{217,218}U$ (lanes 12, 13), or mLBS $C^{204,206,215,217-219}U$ (lanes 14, 15) competitor RNA. Samples were resolved by polyacrylamide gel electrophoresis on a 5% native gel.

effective binding competitors. Wild-type and mutant (m)-LBS RNAs were used as competitors (at concentrations of 10- and 100-fold molar excesses) in RNA gel electrophoretic mobility shift analysis with radiolabeled LR:188−228 RNA, as shown in Figure 9, panel B.

This analysis demonstrated that the rank order of competition of the wild-type and mutant LBS RNAs was: wt LBS, mLBS $C^{217,218}U$, mLBS $C^{215,217-219}U$, mLBS $C^{204,206}U$, and mLBS $C^{204,206,215,217-219}U$. These data suggest that all of the cytidines in the bipartite LBS sequence contribute to the recognition of the lutropin receptor RNA by LRBP-1. However, cytidines 204 and 206 appear most critical for LRBP-1 binding, as mutation of these two nucleotides markedly affected the ability of this RNA to compete for binding of the radiolabeled wild-type LR:188−228 RNA. Additionally, cytidines 217 and 218 appear to be the least important for RNA recognition (compare lanes 9, 10 and 12, 13).

*RNA Electrophoretic Supershift Analysis.* Recently, a cytidine-rich 3′ UTR motif consisting of the sequence (U/C)(C/U)CCCU was identified in the stabilization of tyrosine hydroxylase mRNA during hypoxia in pheochromocytoma (PC12) cells (*23*−*25*). Moreover, this sequence has been

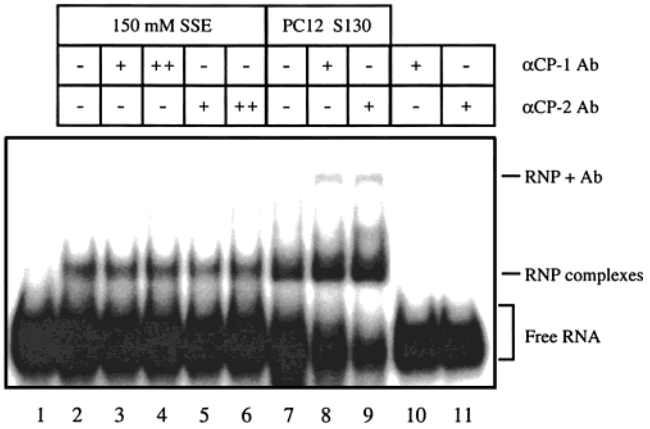


FIGURE 10: RNA gel supershift analysis using αCP-1 and αCP-2 antibodies. Representative autoradiogram of supershift RNA gel electrophoretic mobility shift analysis performed by incubating 2.5 $\times$ $10^4$ cpm of LR:188−228 RNA in the absence (lanes 1, and 10, 11) or presence of 2 $\mu$g of 150 mM KCl S-Sepharose eluate (lanes 2−6) or 40 $\mu$g of PC12 cell S130 (lanes 7−9). Where indicated, antibodies specific for αCP-1 (lanes 3, 4, 8, and 10) or αCP-2 (lanes 5, 6, 9, and 11) were added to the RNA binding reactions. The samples were then resolved by polyacrylamide gel electrophoresis on a 5% native gel at 75 V for 3 h at 4 °C.

shown to bind PC12 cell cytosolic proteins, which were identified as two isoforms of a 40 kDa poly(rC) RNA binding protein, PCBP-1 and -2, also known as αCP-1 and -2, or hnRNP E (*26*). To determine whether LRBP-1 represented one of these poly(rC) RNA binding proteins, supershift RNA gel electrophoretic mobility shift analysis was performed by incubation of LRBP-1 in the 150 mM S-Sepharose eluate with LR:188−228 RNA, followed by incubation with polyclonal antibodies for αCP-1 and αCP-2 (*21*, *22*). As shown in Figure 10, RNA gel electrophoretic mobility supershift analysis was performed by incubation of $5 \times 10^4$ cpm of LR:188−228 RNA with either 5 $\mu$g of 150 mM KCl S-Sepharose eluate (lanes 2−6) or 40 $\mu$g of PC12 cell S130 (lanes 7−9) at 30 °C for 15 min. Polyclonal antibodies for αCP-1 (lanes 3, 4, 8) or αCP-2 (lanes 5, 6, 9) were then added to the binding reactions and incubated for 60 min at 4 °C, followed by polyacrylamide gel electrophoresis on a 5% native gel. As shown in Figure 10, supershifted RNP complexes were not observed in the samples containing LRBP-1, while supershifted species could be observed in samples containing PC12 cell S130 incubated with either αCP-1 or αCP-2 antibodies. This analysis suggested that LRBP-1 does not represent αCP-1 or αCP-2, as no supershifted complexes were observed when antibodies specific for these proteins were incubated with samples containing the 150 mM KCl S-Sepharose eluate.

## DISCUSSION

Control of mRNA turnover as a means to influence steady-state protein levels has been well documented (*27*). The loss of lutropin receptor protein observed during hCG-induced down-regulation is paralleled by the specific loss of steady-state levels of receptor mRNAs in the ovary, which results from an approximate 3-fold decrease in the half-life of receptor mRNA (*6*). Previous work from our laboratory has demonstrated that two proteins isolated from down-regulated rat ovary interacted with lutropin receptor mRNA in a sequence-specific manner (*16*). These two proteins, LRBP-1

and LRBP-2, recognized and bound sequences in the receptor open reading frame between nucleotides 102 and 282. The RNA binding activity of LRBP-1 was further shown to be stimulated by hCG approximately 3-fold during lutropin receptor down-regulation, suggestive of a role in the post-transcriptional regulation of the receptor.

In this report, we have demonstrated that LRBP-1 was partially purified by cation-exchange chromatography. This partially purified LRBP-1 displayed a high degree of specificity in binding of lutropin receptor RNA sequences between nucleotides 188 and 228, with an apparent low nanomolar equilibrium dissociation constant. The low dissociation constant ($K_d$) measured for LRBP-1 binding to LR:188−228 RNA is in the range expected for a specific mRNA binding protein, as has been reported for other RNA binding proteins (*28*). Hydroxyl-radical footprinting demonstrated that within the 41 nucleotide LR:188−228 RNA, LRBP-1 protected a cytidine-rich bipartite sequence of 5′-$U_{203}$CUC-$X_7$-UCUCCCU$_{220}$-3′. More significantly, competitor RNAs containing mutations of distinct cytidines in the regions between 203−206 and 214−220 were able to abolish LRBP-1 RNA binding as shown in Figure 9B. Specifically, mutation of cytidines 204 and 206 markedly decreased competition for wild-type LBS RNA binding by LRBP-1, while RNAs with mutations of cytidines 217 and 218 remained effective binding competitors. Moreover, mutation of all the cytidines in the bipartite LBS abolished LRBP-1 binding. This competition experiment is critical in demonstrating the LBS because both wild-type and mutant LBS RNAs are coincubated with LRBP-1, allowing the protein to discriminate between the two RNAs in solution.

The data presented in this report demonstrate that the protein LRBP-1 specifically binds sequences within the open reading frame of the lutropin receptor mRNA. Studies in several other systems have demonstrated that open reading frame sequences contain trans-acting factor binding sites and contribute to mRNA stability. Two well-studied examples are c-fos and c-myc, which both contain open reading frame protein binding sites in addition to sites in the 3′ UTR. c-fos mRNA contains two open reading frame mRNA stability determinants; one, composed of 320 nucleotides, is located near the center of the mRNA and is sufficient to confer a decrease in stability of globin-fos chimeric mRNAs (*9*, *10*). This region has been additionally shown to be the site of interaction of two proteins, primarily to a purine-rich segment (*8*). The open reading frame of c-myc has also been shown to contribute to the regulation of c-myc mRNA stability by serving as a binding site for an endonuclease, which can be inhibited in vitro by the binding of a polysome-associated protein (*12*, *29*).

Cytosine-rich RNA sequences have also been shown to be involved in the regulation of mRNA stability in several systems. In erythrocytes, α-globin mRNA is stabilized with a half-life of greater than 48 h, which is mediated by three cytidine-rich elements in the 3′ UTR (*30*). A sequence-specific ribonucleoprotein complex has been reported to be formed on the cytidine-rich α-globin 3′ UTR sequences, involving two poly(rC) RNA binding proteins, termed αCP-1 and αCP-2 (*21*, *31*, *32*). Mutation of the cytidines within the three α-globin 3′ UTR binding elements results in destabilization of α-globin mRNA in vivo (*31*). Additionally, the binding of cytidine-rich RNA sequences has been demonstrated to be critical for the stabilization of tyrosine hydroxylase mRNA during hypoxia in PC12 cells (*24*). The core binding element in the 3′ UTR of tyrosine hydroxylase has been shown to be (U/C)(C/U)CCCU, with the underlined nucleotides being most critical for RNA binding (*25*). Czyzyk-Krzeska and colleagues have further demonstrated that this sequence is bound by αCP-1 and αCP-2 (*23*). Interestingly, the lutropin receptor mRNA sequences determined to be critical for LRBP-1 binding contain a near-identical sequence to the tyrosine hydroxylase mRNA sequence bound by αCP-1 and αCP-2. However, when RNA gel electrophoretic mobility supershift analysis was performed using polyclonal antibodies for αCP-1 and αCP-2, no supershifted RNP complexes could be observed with the ovarian 150 mM KCl S-Sepharose eluate, revealing that LRBP-1, isolated from rat ovary, is different from αCP-1 or αCP-2. Accordingly, mutagenesis of the lutropin receptor LBS demonstrated that the cytidines ($C^{217,218}$) which correspond to the critical core binding element in tyrosine hydroxylase mRNA had only a limited effect on disrupting LRBP-1 binding, and appear least important for LRBP-1 binding.

The characterization of the lutropin receptor mRNA sequences contacted by LRBP-1 provides valuable information for future studies directed at defining the putative role of LRBP-1 in the hormonal control of lutropin receptor mRNA stability. Although the mechanism of lutropin receptor mRNA degradation mediated by LRBP-1 remains unknown, we speculate that the control of lutropin receptor mRNA stability could be determined by the ratio of LBS binding by αCP-1 or -2 and LRBP-1. Accordingly, the rate of lutropin receptor mRNA degradation could be modulated by the equilibrium of the stabilizing effects of αCP-1 and -2, and the destabilizing influence of LRBP-1. However, these data do not rule out a more complex model involving other, as yet, unidentified proteins and mRNA sequences. The mechanism by which LRBP-1 regulate lutropin receptor mRNA is currently being investigated using a cell-free mRNA decay system.

## REFERENCES


1. Segaloff, D. L., and Ascoli, M. (1993) *Endocr. Rev. 14*(3), 324−347.
2. McFarland, K. C., Sprengel, R., Phillips, H. S., Kohler, M., Rosemblit, N., Nikolics, K., Segaloff, D. L., and Seeburg, P. H. (1989) *Science 245*, 494−499.
3. LaPolt, P. S., Oikawa, M., Jia, X. C., Dargan, C., and Hsueh, A. J. (1990) *Endocrinology 126*(6), 3277−3279.
4. Hoffman, Y. M., Peegel, H., Sprock, M. J., Zhang, Q. Y., and Menon, K. M. (1991) *Endocrinology 128*(1), 388−393.
5. Peegel, H., Randolph, J., Jr., Midgley, A. R., and Menon, K. M. (1994) *Endocrinology 135*(3), 1044−1051.
6. Lu, D. L., Peegel, H., Mosier, S. M., and Menon, K. M. (1993) *Endocrinology 132*(1), 235−240.
7. Shaw, G., and Kamen, R. (1986) *Cell 46*, 659−667.
8. Chen, C., You, Y., and Shyu, A. B. (1992) *Mol. Cell. Biol. 12*, 5748−5757.
9. Shyu, A., Greenberg, M., and Belasco, J. (1989) *Genes Dev. 3*, 60−72.
10. Shyu, A. B., Belasco, J. G., and Greenberg, M. E. (1991) *Genes Dev. 5*, 221−231.
11. Veyrune, J. L., Carillo, S., Vie, A., and Blanchard, J. M. (1995) *Oncogene 11*(10), 2127−2134.

12. Bernstein, P. L., Herrick, D. J., Prokipcak, R. D., and Ross, J. (1992) *Genes Dev.* (6), 642−654.
13. Alberta, J. A., Rundell, K., and Stiles, C. D. (1994) *J. Biol. Chem. 269*(6), 4532−4538.
14. Wisdon, R., and Lee, W. (1991) *Genes Dev. 5*, 232−243.
15. Port, J. D., Huang, L. Y., and Malbon, C. C. (1992) *J. Biol. Chem. 267*, 24103−24108.
16. Kash, J. C., and Menon, K. M. (1998) *J. Biol. Chem. 273*(17), 10658−10664.
17. Bernard, M. P., Myers, R. V., and Moyle, W. R. (1990) *Mol. Cell. Endocrinol. 71*(3), R19−23.
18. Tso, J. Y., Kao, T. H., Reece, K. S., and Wu, R. (1985) *Nucleic Acids Res. 13*, 2485−2502.
19. Melton, D., Krieg, P. A., Rebagliati, M. R., Maniatis, T., Zinn, K., and Green, M. R. (1984) *Nucleic Acids Res. 12*, 7035−7056.
20. Ansel-McKinney, and Gehrke, L. (1997) *mRNA Formation and Function* (Richter, J. D., Ed.) Academic Press, Inc., San Diego, CA
21. Holcik, M., and Liebhaber, S. A. (1997) *Proc. Natl. Acad. Sci. U.S.A. 94*, 2410−2414.
22. Gamarnik, A. V., and Andino, R. (1997) *RNA 3*, 882−892.
23. Paulding, W., and Czyzyk-Krezeska, M. F. (1999) *J. Biol. Chem. 274*, 2532−2538.
24. Czyzyk-Krzeska, M. F., Dominski, Z., Kole, R., and Millhorn, D. E. (1994) *J. Biol. Chem. 269*(13), 9940−9945.
25. Czyzyk-Krzeska, M., and Beresh, J. E. (1996) *J. Biol. Chem. 271*, 3293−3299.
26. Leffers, H., Dejgaard, K., and Celis, J. E. (1995) *Eur. J. Biochem. 230*, 447−453.
27. Ross, J. (1995) *Microbiol. Rev. 59*(3), 423−450.
28. Burd, C., and Dreyfuss, G. (1994) *Science* (265), 615−621.
29. Prokipcak, R. D., Herrick, D. J., and Ross, J. (1994) *J. Biol. Chem. 269*, 9261−9269.
30. Weiss, I. M., and Liebhaber, S. A. (1995) *Mol. Cell. Biol. 15*, 2457−2465.
31. Kiledjian, M., Wang, X., and Liebhaber, S. A. (1995) *EMBO J. 14*, 4357−4364.
32. Kiledjian, M., DeMaria, C. T., Brewer, G., and Novick, K. (1997) *Mol. Cell. Biol. 17*, 4870−4876.

BI9915770